the plant journal

SEB SOCIETY FOR EXPERIMENTAL BIOLOGY

The Plant Journal (2024) **119**, 2951–2966 doi: 10.1111/tpj.16964

Boosting pro-vitamin A content and bioaccessibility in leaves by combining engineered biosynthesis and storage pathways with high-light treatments

Luca Morelli[1,†,‡], Pablo Perez-Colao[1,†], Diego Reig-Lopez[1], Xueni Di[1], Briardo Llorente[2] and Manuel Rodriguez-Concepcion[1,*]

[1]*Institute for Plant Molecular and Cell Biology (IBMCP), CSIC-Universitat Politècnica de València, Valencia 46022, Spain,*
[2]*ARC Center of Excellence in Synthetic Biology, Australian Genome Foundry, and School of Natural Sciences, Macquarie University, Sydney, New South Wales 2109, Australia*

Received 9 February 2024; revised 16 July 2024; accepted 23 July 2024; published online 9 August 2024.
*For correspondence (e-mail manuelrc@ibmcp.upv.es).
[†]These authors contributed equally to this work.
[‡]Present address: SDU Biotechnology, Faculty of Engineering, University of Southern Denmark, Odense M DK-5230, Denmark

SUMMARY

Biofortification of green leafy vegetables with pro-vitamin A carotenoids, such as β-carotene, has remained challenging to date. Here, we combined two strategies to achieve this goal. One of them involves producing β-carotene in the cytosol of leaf cells to avoid the negative impacts on photosynthesis derived from changing the balance of carotenoids and chlorophylls in chloroplasts. The second approach involves the conversion of chloroplasts into non-photosynthetic, carotenoid-overaccumulating chromoplasts in leaves agroinfiltrated or infected with constructs encoding the bacterial phytoene synthase crtB, leaving other non-engineered leaves of the plant to sustain normal growth. A combination of these two strategies, referred to as strategy C (for cytosolic production) and strategy P (for plastid conversion mediated by crtB), resulted in a 5-fold increase in the amount of β-carotene in *Nicotiana benthamiana* leaves. Following several attempts to further improve β-carotene leaf contents by metabolic engineering, hormone treatments and genetic screenings, it was found that promoting the proliferation of plastoglobules with increased light-intensity treatments not only improved β-carotene accumulation but it also resulted in a much higher bioaccessibility. The combination of strategies C and P together with a more intense light treatment increased the levels of accessible β-carotene 30-fold compared to controls. We further demonstrated that stimulating plastoglobule proliferation with strategy P, but also with a higher-light treatment alone, also improved β-carotene contents and bioaccessibility in edible lettuce (*Lactuca sativa*) leaves.

Keywords: β-carotene, bioaccessibility, biofortification, carotenoids, lettuce, plastoglobules, vitamin A.

INTRODUCTION

Micronutrient deficiency, also known as hidden hunger, is still a major problem in many countries (Fitzpatrick et al., 2012; Díaz-Gómez et al., 2017). In particular, vitamin A deficiency causes xerophthalmia and can lead to other health problems and even death, affecting children from malnourished populations worldwide (Díaz-Gómez et al., 2017; Rodriguez-Concepcion et al., 2018). The incorporation of micronutrients such as vitamin A or its carotenoid precursors as dietary supplements or as food ingredients (i.e., food supplementation or fortification, respectively) can be a solution, but these strategies remain unaffordable in many cases (Fitzpatrick et al., 2012). An alternative approach is the development of crop varieties enriched in micronutrients, that is, biofortification (Morelli & Rodriguez-Concepcion, 2023). Among biofortification strategies, biotechnology has the highest potential for a fast and focused enrichment of the desired plant tissues. In the case of vitamin A, biofortification of rice with β-carotene (the main pro-vitamin A carotenoid) was implemented to create the widely known Golden Rice (Paine et al., 2005; Ye et al., 2000). Further developments have increased β-carotene content in local rice varieties, making the Golden Rice initiative a widely recognized example of biofortification despite the controversies arising from the use of GMOs (Welsch & Li, 2022).

© 2024 The Author(s).
The Plant Journal published by Society for Experimental Biology and John Wiley & Sons Ltd.
This is an open access article under the terms of the Creative Commons Attribution-NonCommercial-NoDerivs License, which permits use and distribution in any medium, provided the original work is properly cited, the use is non-commercial and no modifications or adaptations are made.

Most successful strategies for carotenoid biofortification have been reported in non-photosynthetic tissues, for example, canola seeds, potato tubers, or rice endosperm (Zheng et al., 2020). However, manipulation of carotenoid levels in leaves is much more challenging. Carotenoids participate in light harvesting and are essential for photoprotection in leaves (Lichtenthaler, 2012; Rodriguez-Concepcion et al., 2018). The carotenoid profile of leaf chloroplasts is quite similar in most plant species—with β-carotene accounting for about 20% of total carotenoids—and both composition and levels must be finely balanced with those of chlorophylls for an efficient assembly and functionality of photosynthetic complexes (Domonkos et al., 2013; Esteban et al., 2015; Hashimoto et al., 2018). Low levels of carotenoids are present in the chloroplast envelope membrane, while most carotenoids are associated with proteins in various photosynthetic complexes located in the thylakoid membranes (Domonkos et al., 2013; Hashimoto et al., 2018; Lichtenthaler, 2007). Specifically, β-carotene is primarily associated with photosystems (PSI and PSII) and the cytochrome b6f complex. An increase in β-carotene levels in chloroplasts may hence impact plant photosynthesis (Domonkos et al., 2013; Lichtenthaler, 2012; Mi et al., 2022; Pascal et al., 2005).

In some plants, carotenoids provide yellow to red colors to non-photosynthetic tissues such as carrot roots, marigold flowers and tomato ripe fruits (Rodriguez-Concepcion et al., 2018). Unlike chloroplasts, the carotenoid-accumulating plastids found in these tissues—called chromoplasts—have a very diverse carotenoid composition. Chromoplasts naturally differentiate from different types of plastids, including chloroplasts (Sadali et al., 2019; Sun et al., 2018). While they do not normally develop in leaves, recent results have demonstrated that leaf chloroplasts can be artificially converted into chromoplasts by overexpressing a bacterial phytoene synthase enzyme—crtB—that catalyzes the first committed step of the carotenoid pathway (Llorente et al., 2020). Artificial leaf chromoplasts accumulate higher levels of carotenoids and are particularly enriched in β-carotene (Llorente et al., 2020; Morelli, Torres-Montilla, et al., 2023). The formation of chromoplasts (natural or artificial) involves the development of internal structures that sequester and store carotenoids (Sadali et al., 2019; Sun et al., 2018; Torres-Montilla & Rodriguez-Concepcion, 2021). Carotenoid-storing structures differ among chromoplasts depending on the carotenoid content, tissue, or plant species. For example, tomato fruit chromoplasts accumulate β-carotene in plastoglobules (PGs), whereas carrot root chromoplasts accumulate much higher concentrations of β-carotene in crystalline bodies (Kim et al., 2010; Schweiggert et al., 2012). In leaves, PGs proliferate after exposure to high light intensity (Lichtenthaler, 2007) or when chloroplasts are differentiated into chromoplasts upon crtB expression (Morelli, Torres-Montilla, et al., 2023). PGs are actually the main site for β-carotene production and storage in artificial chromoplasts (Morelli, Torres-Montilla, et al., 2023).

In plant cells, carotenoids are synthesized from the five-carbon (C_5) isoprenoid precursors isopentenyl diphosphate (IPP) and its isomer dimethylallyl diphosphate (DMAPP) produced by the plastidial methylerythritol 4-phosphate (MEP) pathway (Rodríguez-Concepción & Boronat, 2002). Condensation of three IPP and one DMAPP molecules forms C_{20} geranylgeranyl diphosphate (GGPP), the direct precursor for carotenoids and other plastidial isoprenoids such as diterpenes, chlorophylls, tocopherols, plastoquinones, and phylloquinones (Figure 1). The first committed step of the plant carotenoid pathway is the formation of C_{40} phytoene from two molecules of GGPP catalyzed by the enzyme phytoene synthase (PSY in plants, crtB in bacteria). Colorless phytoene is then sequentially desaturated and isomerized to lycopene, the red pigment typical of ripe tomato fruit. Cyclization of the two ends of the linear lycopene molecule generates β-carotene (with two β rings) or α-carotene (with one ε ring and one β ring). The formation of two ε rings is very rare in plant carotenoids, although there are examples in crops such as lactucaxanthin in lettuce (Britton, 1995; Phillip & Young, 1995). Oxidative modification of the rings generates oxygenated carotenoids—known as xanthophylls—such as violaxanthin and neoxanthin (from β-carotene) or lutein (from α-carotene, an intermediate that is hardly detected in chloroplasts). The same precursors used for carotenoid biosynthesis in plastids, IPP, and DMAPP, are also produced in the cytosol by the mevalonate (MVA) pathway (Rodríguez-Concepción & Boronat, 2015). MVA-derived IPP and DMAPP are mostly used to produce polyterpenes, sesquiterpenes, and triterpenes such as phytosterols (usually, the major product of the pathway), while much lower levels of GGPP are synthesized for the biosynthesis of diterpenes and protein prenylation. Interestingly, cytosolic IPP and DMAPP can be used to produce carotenoids by introducing bacterial or fungal enzymes that produce GGPP and convert it into downstream carotenoids (Figure 1; Andersen et al., 2021; Majer et al., 2017; Zheng et al., 2023). In particular, very high levels of extraplastidial lycopene were produced by combining constructs encoding a truncated version of hydroxymethylglutaryl CoA reductase (tHMGR) to increase the MVA pathway flux, crtE to produce GGPP from MVA-derived IPP and DMAPP, a cytosolic version of the crtB enzyme (c-crtB) to transform GGPP into phytoene, and crtI to synthesize lycopene from phytoene (Figure 1A; Andersen et al., 2021). Producing carotenoids in the cytosol preserves the chloroplast carotenoid profile without disrupting the photosynthetic complexes and allows the accumulation of carotenoid intermediates by separating them from the endogenous (plastidial) enzymes that convert them into downstream

© 2024 The Author(s).

1365313x, 2024, 6, Downloaded from https://onlinelibrary.wiley.com/doi/10.1111/tpj.16964 by Universitat Politecnica De Valencia, Wiley Online Library on [19/09/2024]. See the Terms and Conditions (https://onlinelibrary.wiley.com/terms-and-conditions) on Wiley Online Library for rules of use; OA articles are governed by the applicable Creative Commons License

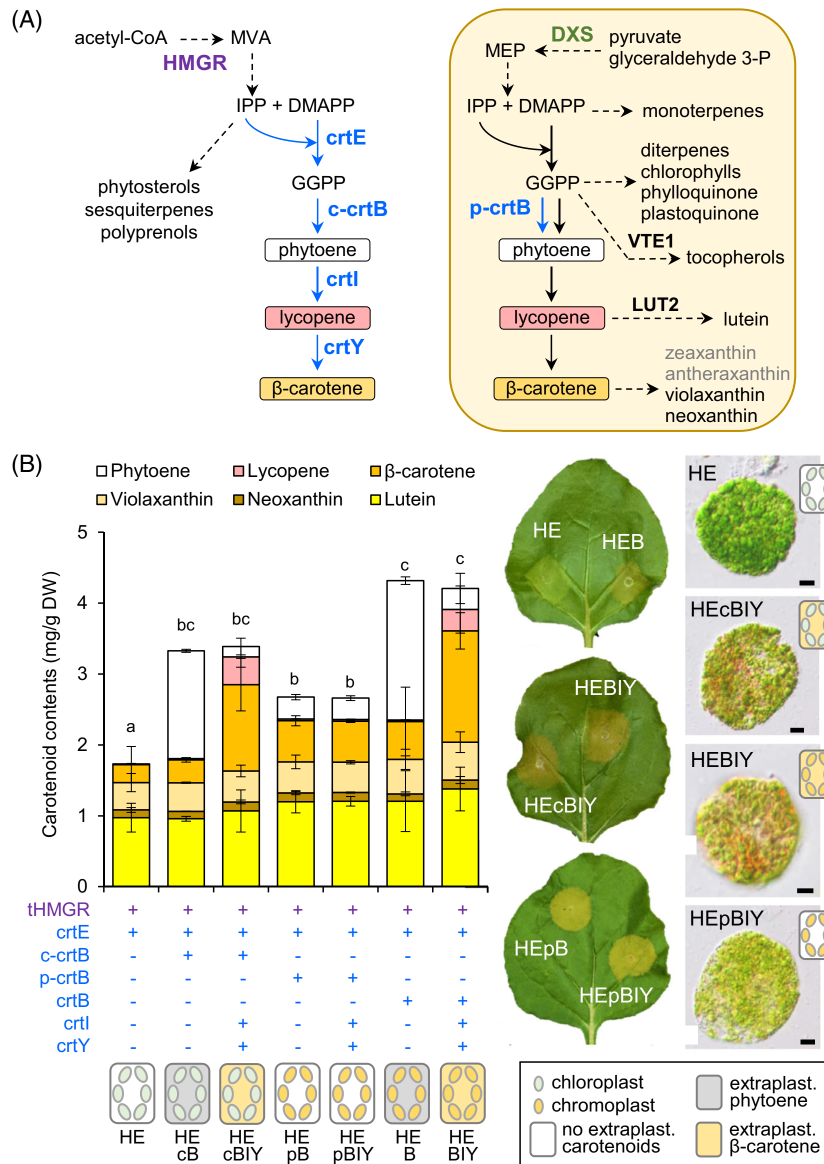

Figure 1. Strategies to produce β-carotene in different cell compartments.
(A) Schematic representation of the carotenoid biosynthetic pathways and enzymes covered in this work. Dashed arrows represent multiple steps. The plastidial pathway is boxed in orange.
(B) Carotenoid levels in *N. benthamiana* leaves 6 days after agroinfiltration with combinations containing (+) or not (−) the indicated constructs. To name the combinations, construct nomenclature was abbreviated as follows: tHGMR (H), crtE (E), c-crtB (cB), p-crtB (pB), crtB (B), crtI (I), and crtY (Y). For example, the combination referred to as HEcB included tHMGR, crtE, and c-crtB. Mean and SD of $n \geq 3$ independent biological replicates are shown. DW, dry weight. Letters represent statistically significant differences ($P < 0.05$) among means of total carotenoid levels. Representative images of leaves agroinfiltrated with the indicated combinations and protoplasts isolated from the agroinfiltrated areas (bar, 10 μm) are also shown. Cartoons are a schematic representation of the subcellular sites of carotenoid accumulation.

carotenoid end-products. Extraplastidial carotenoids can form crystals (Andersen et al., 2021) or localize in cytosolic lipid droplets—CLDs—(Zheng et al., 2023) similar to those found in yeast strains engineered to overaccumulate carotenoids (Bu et al., 2022) or in microalgae that naturally produce these lipophilic compounds in the cytosol (Ezzedine et al., 2023; Pick et al., 2019).

Here, we explored several strategies to biofortify leaves of the model plant *Nicotiana benthamiana* and the crop plant lettuce (*Lactuca sativa*) with β-carotene. We confirmed that extraplastidial carotenoids were sequestered in cytosolic crystalline and CLD-like structures similar to those found in chromoplasts, suggesting that carotenoid storage structures are not developmentally controlled but develop

© 2024 The Author(s).

1365313x, 2024, 6, Downloaded from https://onlinelibrary.wiley.com/doi/10.1111/tpj.16964 by Universitat Politecnica De Valencia, Wiley Online Library on [19/09/2024]. See the Terms and Conditions (https://onlinelibrary.wiley.com/terms-and-conditions) on Wiley Online Library for rules of use; OA articles are governed by the applicable Creative Commons License

as a response to sudden overaccumulation of these lipophilic compounds. Furthermore, we tested different metabolic, genetic, and chemical (hormone treatment) approaches to improve plastidial β-carotene accumulation in plastids and found that promoting the proliferation of PGs with intense light treatments improved both β-carotene accumulation and bioaccessibility to unprecedented levels.

RESULTS

An engineered cytosolic pathway for β-carotene production

To produce β-carotene in the cytosol, *Nicotiana benthamiana* leaves were agroinfiltrated with constructs encoding cytosolic versions of biosynthetic enzymes, including the *Pantoea ananatis* lycopene-β-cyclase crtY (Figure 1A). The resulting construct combination was named HEcBIY because it included tHMGR (in short, H), crtE (E), c-crtB (cB), crtI (I), and crtY (Y). Parallel experiments were carried out with combinations of tHMGR + crtE (named HE) and tHMGR + crtE + c-crtB (named HEcB). HPLC analysis of leaf samples collected at 6 days post-infiltration (dpi) showed that total carotenoid levels were more than doubled when c-crtB was included in the combination (Figure 1B). As expected, the main carotenoids were phytoene and β-carotene in HEcB and HEcBIY leaves, respectively (Figure 1B). The accumulation of β-carotene in HEcBIY leaves (corresponding to the sum of chloroplast levels plus engineered cytosolic contents) was about 4-fold higher than the levels measured in HE leaves (corresponding to only chloroplast levels) (Figure 1B). The relatively high amount of lycopene remaining in HEcBIY leaf sectors explains their reddish color (Figure 1B). Protoplasts isolated from agroinfiltrated HEcBIY cells showed a pigmented cytosol (Figure 1B), confirming that carotenoids were produced in this cell compartment.

Cytosolic production of carotenoids can be combined with chromoplast development for further carotenoid enrichment of leaves

Agroinfiltration of *N. benthamiana* leaves with combinations containing a plastid-targeted crtB enzyme (herein referred to as p-crtB) led to the development of yellowish chromoplasts and a *ca.* 2-fold increase in β-carotene levels compared to control samples harboring green chloroplasts without p-crtB (Figure 1B). We next tested whether triggering plastidial overaccumulation of β-carotene (that we name here strategy P) could be combined with the cytosolic production of β-carotene (that we called strategy C) just by using the unmodified crtB enzyme, which is known to act in both cytosolic and plastidic compartments (Andersen et al., 2021; Llorente et al., 2020). A comparison of unmodified crtB (B), c-crtB (cB), or p-crtB (pB) in combination with tHMGR (H) and crtE (E) showed that the content of phytoene measured in leaf sectors producing the untargeted crtB protein (HEB) was roughly a sum of the amounts obtained with the cytosolic (HEcB) plus the plastidial (HEpB) enzymes (Figure 1B). An additive phenotype was also observed for β-carotene when comparing HEBIY with HEcBIY plus HEpBIY (Figure 1B). The levels of β-carotene in HEBIY samples increased about 5-fold compared to HE controls (Figure 1B). Protoplasts isolated from agroinfiltrated HEBIY cells showed a reddish cytosol (similar to that in HEcBIY protoplasts) and yellow plastids (similar to those found in HEpBIY protoplasts), consistent with the predicted distribution of carotenoid pigments in these cells (Figure 1B).

Cytosolic carotenoids are sequestered in crystalline and globular structures like those found in chromoplasts

To investigate the extraplastidial carotenoid accumulation sites in HEcBIY and HEBIY cells, we analyzed their ultrastructure using transmission electron microscopy (TEM) (Figure 2). Electron-dense vesicles (EVs) similar to CLDs were found in the cytosol of HEcBIY and HEBIY but not in control cells (Figure 2A–D). In some cases, clusters of EVs were located next to undulating membranes (UMs) that resembled the remnants of lycopene crystal envelopes typical of tomato ripe fruit chromoplasts (Figure 2C). UMs were also detected separately from EVs (Figure 2D). As expected, HEcBIY cells harbored chloroplasts similar to those in control cells (Figure 2A,B), whereas HEBIY cells contained chromoplasts in different stages of transformation (Figure 2D,E).

Providing more plastidial precursors does not improve carotenoid production due to a bottleneck at the phytoene desaturation level

To improve carotenoid production with strategy P, we used the enzyme deoxyxylulose 5-phoshate synthase (DXS), which catalyzes the first and main rate-determining step of the MEP pathway (Rodríguez-Concepción & Boronat, 2015). *N. benthamiana* leaves were agroinfiltrated with constructs for crtB and DXS sequences from Arabidopsis (AtDXS) and tomato (SlDXS1 and SlDXS2). Of the three isoforms, only SlDXS1 led to a statistically significant increase in total carotenoid levels compared to crtB samples (Figure 3A). Such an increase was mainly due to a massive accumulation of phytoene (Figure 3A), which resulted in a faster drop of the effective quantum yield of photosystem II (ϕPSII) as chloroplasts turned into chromoplasts (Figure 3B). No improvement in the contents of β-carotene or any other plastidial carotenoid besides phytoene was observed when SlDXS1 was incorporated into the HEBIY combination (Figure 3C and Table 1).

Exploring other ways to promote artificial chromoplast differentiation

We next explored the possibility of increasing leaf β-carotene contents by promoting crtB-mediated artificial chromoplastogenesis following a pharmacological and a

1365313x, 2024, 6, Downloaded from https://onlinelibrary.wiley.com/doi/10.1111/tpj.16964 by Universitat Politecnica De Valencia, Wiley Online Library on [19/09/2024]. See the Terms and Conditions (https://onlinelibrary.wiley.com/terms-and-conditions) on Wiley Online Library for rules of use; OA articles are governed by the applicable Creative Commons License

1365313x, 2024, 6, Downloaded from https://onlinelibrary.wiley.com/doi/10.1111/tpj.16964 by Universitat Politecnica De Valencia, Wiley Online Library on [19/09/2024]. See the Terms and Conditions (https://onlinelibrary.wiley.com/terms-and-conditions) on Wiley Online Library for rules of use; OA articles are governed by the applicable Creative Commons License

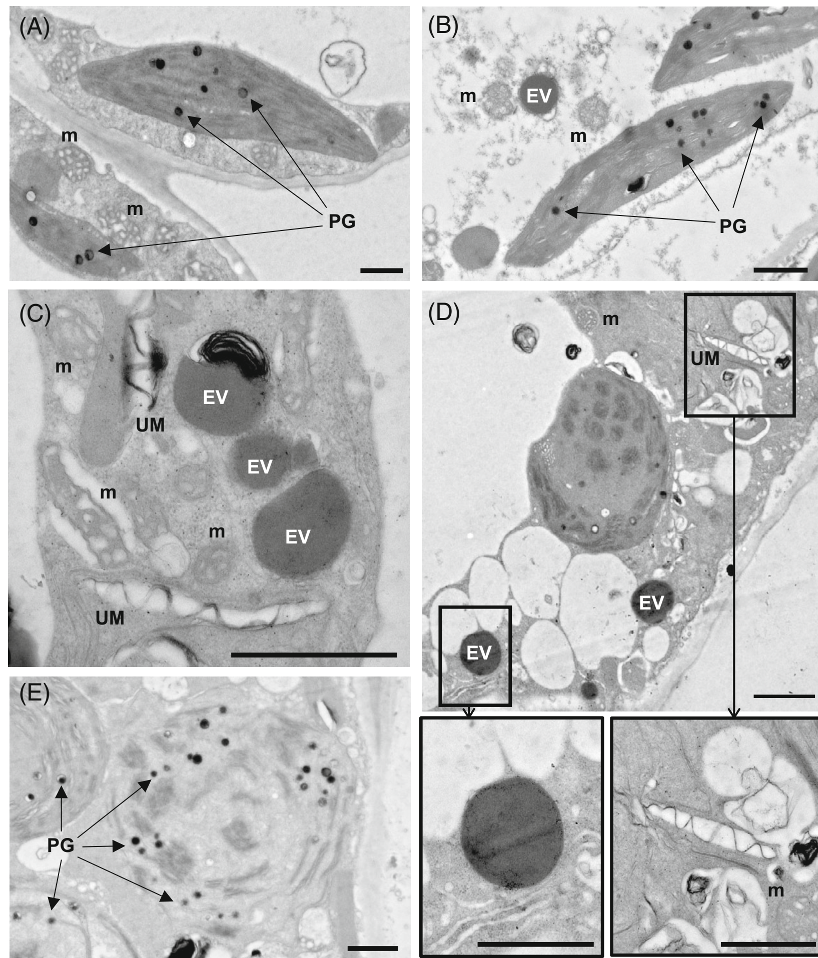

Figure 2. Carotenoids produced in the cytosol accumulate in structures like those found in chromoplasts.
Images show transmission electron microscopy (TEM) images of representative areas from *Nicotiana benthamiana* leaves agroinfiltrated with constructs harboring a GFP control (A) or combinations HEcBIY (B, C) or HEBIY (D, E) and collected at 6 dpi (see Figure 1 caption for the nomenclature of construct combinations). EV, electron-dense vesicles; m, mitochondria; PG, plastoglobules; UM, undulating membrane. Bar, 1 μm.

genetic strategy. For the former, we reasoned that the exogenous application of phytohormones could positively (or negatively) impact the formation of artificial chromoplasts resulting in higher (or lower) β-carotene levels. Most plant hormones tested (Table 2) had no effect on the speed of chloroplast-to-chromoplast transformation (estimated as ϕPSII drop rate) compared to leaves treated with a mock solution (Figure 4A). The only exceptions were gibberellins (gibberellic acid, GA_3), which accelerated the chromoplastogenesis process, and synthetic strigolactones (GR24) and auxins (picloram), which delayed it (Figure 4A). In particular, the application of GA_3 resulted in a significant decrease of ϕPSII in p-crtB samples at 36 hpi compared to the mock control (Figure 4A), eventually leading to a higher content of carotenoids, including β-carotene (Figure 4B). By contrast, leaves treated with GR24 or picloram showed significantly higher ϕPSII from 48 hpi (Figure 4A) and lower levels of carotenoids at 96 hpi (Figure 4B). To test whether the internal amounts of these phytohormones could regulate the chromoplastogenesis process, we used inhibitors of the endogenous biosynthesis pathways (Table 2). However, none of these inhibitors had any significant effect on ϕPSII or carotenoid contents compared to plants treated with the mock solution (Figure 4).

Finally, we tested a genetic approach based on the use of Arabidopsis mutants in plastid-to-nucleus (i.e., retrograde) communication or in biosynthetic steps competing with β-carotene biosynthesis (Figure 5). Soil-grown wild-type (WT) and mutant plants were infected with the viral vector TuMV-crtB and the levels of carotenoids were measured 3 weeks later, when symptoms (leaves turning vivid yellow) were obvious. None of the retrograde mutants analyzed (*gun1*, *sal1*, and *csb3*) showed significant changes in their carotenoid profile (Figure 5A) or β-carotene content (Figure 5B) compared to WT controls. In the case of biosynthetic mutants, we used the tocopherol

© 2024 The Author(s).
The Plant Journal published by Society for Experimental Biology and John Wiley & Sons Ltd.,

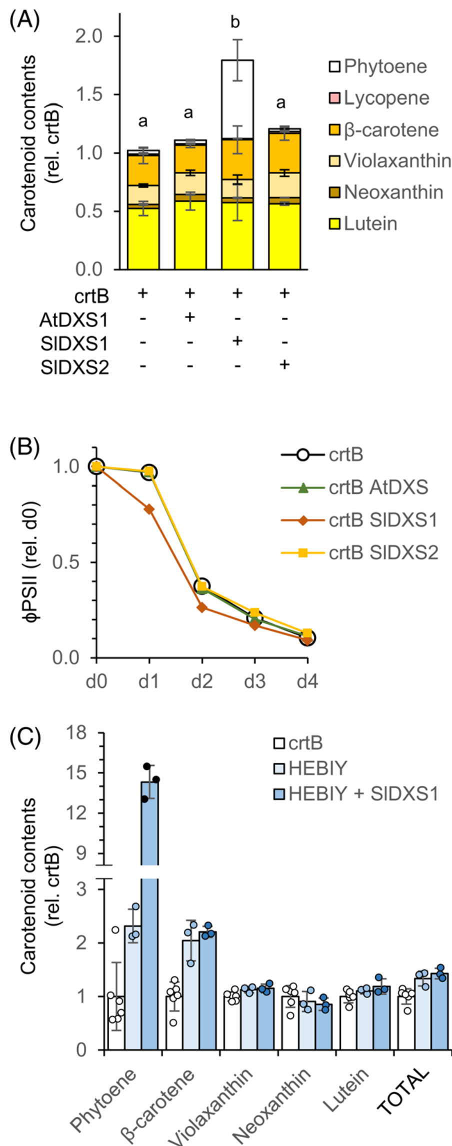

Figure 3. Increased supply of plastidial precursors results in phytoene overaccumulation.
N. benthamiana leaves were agroinfiltrated with combinations containing (+) or not (−) the indicated constructs and analyzed at 6 dpi (see Figure 1 caption for the nomenclature of construct combinations). (A) Relative carotenoid levels are shown as the mean and SD of $n \geq 3$ independent biological replicates. Letters represent statistically significant differences ($P < 0.05$) among means of total carotenoid levels.
(B) Relative effective quantum yield of photosystem II (ϕPSII). Mean and SD of at least 5 measurements in $n \geq 3$ independent leaf samples are expressed relative to day 0 values.
(C) Relative levels of the indicated carotenoids are represented as individual values (dots) and the corresponding mean and SD.

biosynthesis mutant *vte1* to decrease competition for GGPP and the lycopene ε cyclization mutant *lut2* to block the β, ε branch of the carotenoid pathway leading to lutein and hence divert all precursors to the β-carotene branch (Figure 1A). TuMV-crtB-infected yellow (i.e., chromoplast-containing) leaf tissues of WT and mutant plants contained similar levels of total carotenoids (Figure 5A), but a modest (1.5-fold) enrichment in β-carotene contents was found in the *lut2* mutant (Figure 5B).

Exposure to more intense light is an effective strategy to further enrich leaves in β-carotene

Exposure to increasing light intensity was implemented to stimulate the proliferation of PGs and analyze the concomitant effect on β-carotene production and storage in artificial chromoplasts (Figure 6). *N. benthamiana* plants grown under control light conditions (50 μmol photons m^{-2} sec^{-1} white light, namely W50) were exposed for 3 days to 10-fold higher light intensity (500 μmol photons m^{-2} sec^{-1} white light, W500) or kept under W50. Then, leaves from the two sets of plants were agroinfiltrated with the HEBIY combination, and plants were kept under W50 until samples were taken for HPLC analysis at 6 dpi (Figure 6). Leaves pre-treated with W500 showed a higher content of β-carotene and total carotenoids compared to leaves sampled from control plants grown under W50 (Figure 6A). Together, combining strategies C and P with W500 treatment resulted in almost a 3-fold increase in total carotenoid levels but a more than 7-fold increase in β-carotene (pro-vitamin A) contents of *N. benthamiana* leaves compared to controls agroinfiltrated with the GFP protein (Figure 6B). Indeed, the proportion of β-carotene relative to total leaf carotenoids was raised from around 20% in the chloroplasts of GFP control leaves to 30% in the chromoplasts of crtB samples and 45% in HEBIY leaves exposed to W500 (Figure 6B).

Accumulation of β-carotene in PGs and extraplastidial locations increases its bioaccessibility

The fraction of a nutrient (e.g., a carotenoid) accessible for absorption is referred to as bioaccessibility. We observed that the bioaccessibility of the β-carotene engineered in the cytosol (HEcBIY samples) was only marginally higher compared to that produced and stored in chloroplasts (HE samples) (Figure 7). Interestingly, the induction of chromoplastogenesis significantly increased the bioaccessibility of β-carotene (Figure 7). Next, we promoted PG proliferation by exposure to W500 similarly to that described above and then calculated bioaccessibility in p-crtB and HEBIY leaves at 6 dpi (Figure 7). W500 treatment resulted in increased β-carotene bioaccessibility in both p-crtB and HEBIY samples, but it was statistically significant only in the case of p-crtB, likely because the bioaccessibility of the large amount of extraplastidial β-carotene found in HEBIY samples hardly changes (Figure 7). Considering both amount and bioaccessibility, the combination of strategies C and P together with the light treatment (HEBIY + W500) resulted in an impressive 30-fold increase in the contents of accessible β-carotene compared to HE controls (Figure 7).

© 2024 The Author(s).

1365313x, 2024, 6, Downloaded from https://onlinelibrary.wiley.com/doi/10.1111/tpj.16964 by Universitat Politecnica De Valencia, Wiley Online Library on [19/09/2024]. See the Terms and Conditions (https://onlinelibrary.wiley.com/terms-and-conditions) on Wiley Online Library for rules of use; OA articles are governed by the applicable Creative Commons License

Table 1 Absolute levels of carotenoids in agroinfiltrated *N. benthamiana* leaves

Combination	Phytoene	β-carotene	Violaxanthin	Neoxanthin	Lutein	Total
crtB	0.079 ± 0.050	0.639 ± 0.172	0.400 ± 0.034	0.084 ± 0.017	1.291 ± 0.150	2.463 ± 0.350
HEBIY	0.182 ± 0.024	1.306 ± 0.243	0.451 ± 0.024	0.076 ± 0.016	1.425 ± 0.071	3.287 ± 0.343
HEBIY + SlDXS1	1.126 ± 0.097	1.409 ± 0.066	0.461 ± 0.032	0.072 ± 0.010	1.532 ± 0.187	3.514 ± 0.244

Samples correspond to those represented in Figure 3C. Numbers indicate mean ± SD (mg of carotenoid per g of dry weight of leaf tissue).

Table 2 Compounds applied to test hormonal regulation of artificial chromoplast development in *N. benthamiana* leaves

Class	Type	Compound	Acronym	Concentration (μM)
Hormone	Brassinosteroid	Epibrassinolide	EBR	10
	Cytokinin	2-Isopentenyladenine	2iP	10
	Abscisic acid	Abscisic acid	ABA	10
	Jasmonate	Methyl jasmonate	MeJA	100
	Salicylic acid	Salycilic acid	SA	300
	Gibberellin	Giberellic acid	GA3	100
Synthetic hormone	Strigolactone analog	GR24	GR24	100
	Auxin analog	Picloram	PIC	50
Hormone donor	Nitric oxide donor	Sodium nitroprusside	SNP	100
	Ethylene donor	Etephon	ETH	1500
Hormone synthesis inhibitor	Gibberellin inhibitor	Paclobutrazol	PAC	10
	Strigolactone inhibitor	4-Hydroxyaryl hydroxamic acid	D2	100
	Auxin inhibitor	L-Kynurenine	L-Kyn	500

All the compounds were diluted in 0.05% Tween20 (in water) to the indicated concentration before application to the leaf surface with a fine brush.

Developed strategies can be applied to the biofortification of edible lettuce leaves

To investigate whether the described approaches could also be extended to lettuce, leaves of the Romaine variety were infected with LMV-crtB, a viral vector carrying crtB (Figure 8). About 2 weeks later, LMV-crtB leaves had developed a characteristic orange/yellow color and a strong increase in their carotenoid content compared to control leaves infected with an empty vector (LMV), which showed a normal green color but very curly leaves as expected from viral infection (Figure 8A). The characteristic lettuce carotenoid lactucaxanthin also increased in LMV-crtB samples, confirming a general upregulation of the whole carotenoid pathway (Figure 8B). Similar to that described in the *N. benthamiana* system, crtB also promoted the development of PGsϕ in lettuce, as deduced from the increased levels of PG-associated fibrillins FBN1a and FBN2 in LMV-crtB samples compared to LMV controls (Figure 8C).

We next tested whether carotenoid accumulation and accessibility may improve after exposing W50-grown lettuce plants to higher light intensity (W500). Again coherently with what was observed in *N. benthamiana* leaves (Figure 7), W500 treatment caused an increase in total carotenoids in general and β-carotene in particular (Figure 8B). Interestingly, such carotenoid biofortification also took place in the chloroplasts of non-engineered control leaves. Bioaccessibility of β-carotene also improved substantially in leaves exposed to higher light regardless of whether they were harboring chloroplasts (LMV) or chromoplasts (LMV-crtB), even though the highest levels were detected when crtB and W500 treatments were combined (Figure 8B). In terms of increasing accessible β-carotene contents, the treatment with more intense light worked better than the use of crtB (strategy P), and the highest levels were achieved when combining both approaches (Figure 8D).

DISCUSSION

Biofortification of green leafy vegetables with pro-vitamin A carotenoids is still in its infancy, in part because of the challenges associated with changing the balance between carotenoids and chlorophylls in chloroplasts and hence negatively impacting photosynthesis (Domonkos et al., 2013; Esteban et al., 2015; Hashimoto et al., 2018; Zhen & van Iersel, 2017; Zheng et al., 2020). Here, we present two strategies that can be used separately or combined to overcome this problem. Strategy C involved producing pro-vitamin A carotenoids such as β-carotene in extraplastidial locations to avoid disrupting the balance of photosynthetic pigments and hence interfering with photosynthesis. Strategy P was implemented by triggering the conversion of chloroplasts into chromoplasts. In

© 2024 The Author(s).

1365313x, 2024, 6, Downloaded from https://onlinelibrary.wiley.com/doi/10.1111/tpj.16964 by Universitat Politecnica De Valencia, Wiley Online Library on [19/09/2024]. See the Terms and Conditions (https://onlinelibrary.wiley.com/terms-and-conditions) on Wiley Online Library for rules of use; OA articles are governed by the applicable Creative Commons License

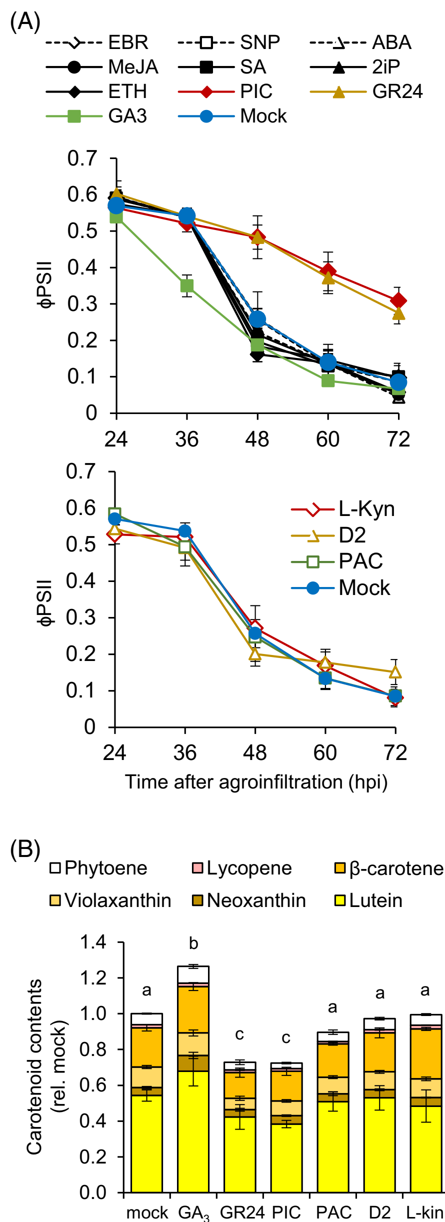

Figure 4. Treatment with some phytohormones interferes with the chromoplastogenesis process.
N. benthamiana leaves agroinfiltrated with the p-crtB construct were treated with the indicated compounds or a mock solution.
(A) Effective quantum yield of photosystem II (ϕPSII) values in leaf areas treated with the indicated phytohormones (upper plot), or inhibitors (lower plot). Hormone treatments that had no effect compared to the mock treatment are shown in black in the upper plot. Mean and SD of at least 5 measurements in $n \geq 3$ independent leaves are shown.
(B) Relative carotenoid levels at 96 hpi are shown as the mean and SD of $n \geq 3$ independent biological replicates. Letters represent statistically significant differences ($P < 0.05$) among means of total carotenoid levels. See Table 2 for the full names, type, and class of the compounds and concentrations used.

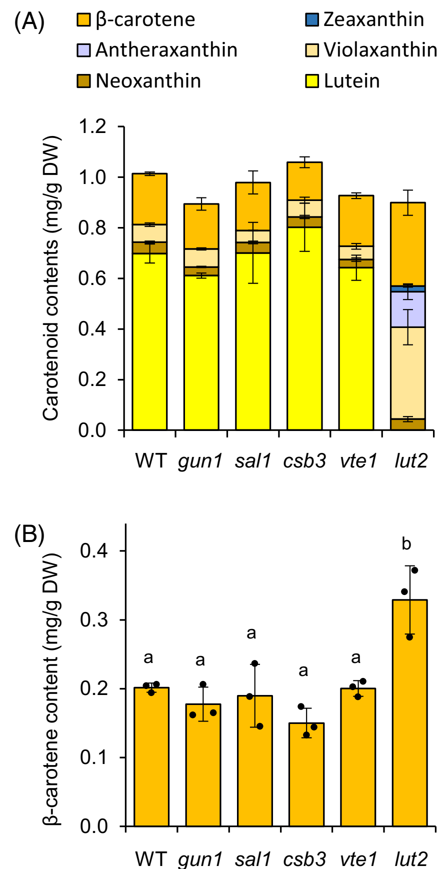

Figure 5. Genetic manipulations of retrograde and carotenoid-related pathways hardly impact β-carotene levels.
Arabidopsis wild-type (WT) plants and the indicated mutants were infected with the TuMV-crtB vector. After 3 weeks, rosette leaves showing the phenotypes associated with viral infection (e.g., curled leaves) and ctrB activity (e.g., yellow leaves) were collected to measure carotenoid contents.
(A) Mean and SD of total carotenoid levels of $n = 3$ samples from different plants.
(B) Relative levels of β-carotene in the samples are shown in (A). Dots represent individual values and letters represent statistically significant differences ($P < 0.05$) among means.

combination with intense light treatments, an impressive (about 30-fold) increase in bioaccessible β-carotene content was achieved in leaves (Figure 7). Furthermore, we show that the generated knowledge can be steadily translated to biofortify green leafy vegetables such as lettuce (Figure 8). Improving the levels, storage, and bioaccessibility of carotenoids in lettuce has the added advantage of providing an increased source of lactucaxanthin, a unique ε, ε-carotenoid reported to have antidiabetic and antioxidant properties (Gopal et al., 2017).

The 2-fold increase in total carotenoid levels and 4-fold increase in β-carotene contents achieved by strategy C

© 2024 The Author(s).

1365313x, 2024, 6, Downloaded from https://onlinelibrary.wiley.com/doi/10.1111/tpj.16964 by Universitat Politecnica De Valencia, Wiley Online Library on [19/09/2024]. See the Terms and Conditions (https://onlinelibrary.wiley.com/terms-and-conditions) on Wiley Online Library for rules of use; OA articles are governed by the applicable Creative Commons License

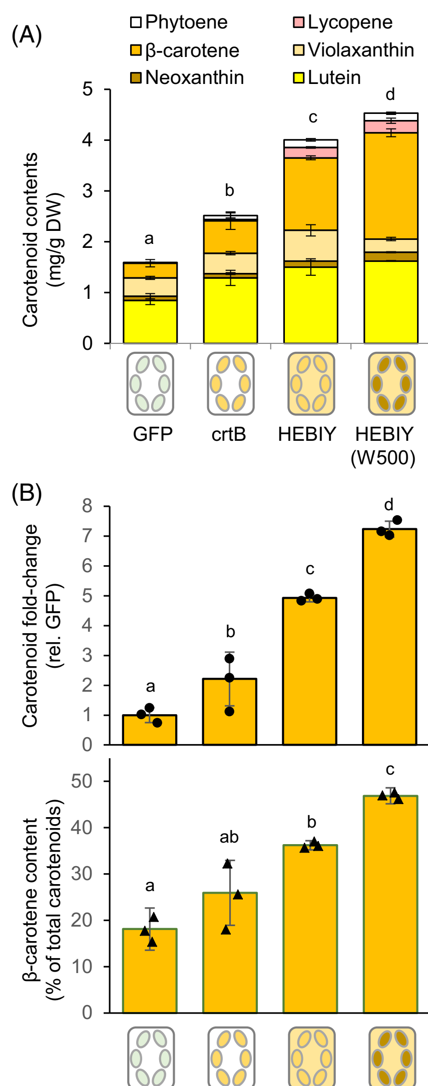

Figure 6. Exposure to high irradiances further increases β-carotene levels. *N. benthamiana* plants grown under normal light conditions (W50) were exposed for 3 days to 10-fold higher light intensity (W500) or kept under W50. Then, leaves from the two sets of plants were agroinfiltrated with the indicated construct combinations and analyzed at 6 dpi (see Figure 1 caption for the nomenclature of construct combinations).
(A) Absolute carotenoid levels are shown as the mean and SD of $n = 3$ independent biological replicates.
(B) Relative levels of β-carotene in the samples shown in (A). The upper plot represents the contents relative to those in control (GFP) samples, whereas the lower plot shows the proportion relative to total carotenoids in every combination. Dots represent individual values and letters indicate statistically significant differences ($P < 0.05$) among means.

in *N. benthamiana* confirms a remarkable capacity of leaf cells to accumulate carotenoids outside chloroplasts. The precise location where extraplastidial β-carotene is synthesized is unknown, but the presence of cytosolic lipid vesicles (EVs) and crystal remnants (UMs) in engineered plant cells (Figure 2; Zheng et al., 2023) very similar to carotenoid-sequestering structures found in chromoplasts (Nogueira et al., 2013; Sadali et al., 2019; Sun et al., 2018; Torres-Montilla & Rodriguez-Concepcion, 2021) strongly suggests that they are sites of carotene accumulation. UMs usually form when the membranes that cover the crystalline carotenoid structures shrink as the dehydration step of the TEM sample preparation results in the loss of the crystals. The UMs found in HEcBIY and HEBIY cells might correspond to lycopene, a carotenoid known to form cytosolic crystals in HEcBI cells (Andersen et al., 2021). However, the observation that β-carotene bioaccessibility does not substantially improve in HEcBIY leaves compared to HE controls (Figure 7) suggests that crystals might actually correspond to poorly bioaccessible β-carotene, which might counterbalance the higher bioaccessibility expected for vesicle-associated β-carotene (Jeffery, Holzenburg, & King, 2012; Jeffery, Turner, & King, 2012). Because the vesicles (EVs) are more abundant than the crystal remnants, we speculate that crystallization only occurs at locations where high β-carotene concentrations are achieved. In any case, the unprecedented observation of different structures for carotenoid storage coexisting in cellular compartments that do not normally store these pigments (e.g., the cytosol of plant cells) demonstrates that they do not differentiate as part of a pre-established developmental program but develop as a response to sudden overaccumulation of lipids (e.g., carotenoids). Furthermore, our results provide strong evidence that environmental factors (e.g., carotenoid type or accumulation level) rather than genetically determined cues are the main trigger for the development of specific storing structures (i.e., crystalline, globular, etc.). Besides improving storage, our data suggest that other factors might be more limiting to further increase the contents of this pro-vitamin A carotenoid in the cytosol. In particular, high levels of residual lycopene and phytoene that are not converted into β-carotene (Figure 1B) suggest that crtI and crtY activities are important limiting steps. These bacterial enzymes likely interact to form a multiprotein complex that facilitates substrate channeling (Nogueira et al., 2013; Ravanello et al., 2003). Engineering a scaffolding system to get all the carotenoid mini-pathway enzymes together might contribute to improve substrate delivery and product release, eventually resulting in higher β-carotene titers. Alternatively, the use of directed evolution to create crtI and crtY enzymes optimized to work in a plant cytosolic environment might contribute to improve the corresponding enzymatic conversions.

A bottleneck has also been unveiled in the case of strategy P. Upregulation of the MEP pathway flux by overexpressing the tomato *SlDXS1* gene resulted in a high increase in the level of phytoene but no significant increase in downstream carotenoids (Figure 3). Besides confirming that SlDXS1 works to increase the MEP pathway flux, this result also suggested that the endogenous

© 2024 The Author(s).

1365313x, 2024, 6, Downloaded from https://onlinelibrary.wiley.com/doi/10.1111/tpj.16964 by Universitat Politecnica De Valencia, Wiley Online Library on [19/09/2024]. See the Terms and Conditions (https://onlinelibrary.wiley.com/terms-and-conditions) on Wiley Online Library for rules of use; OA articles are governed by the applicable Creative Commons License

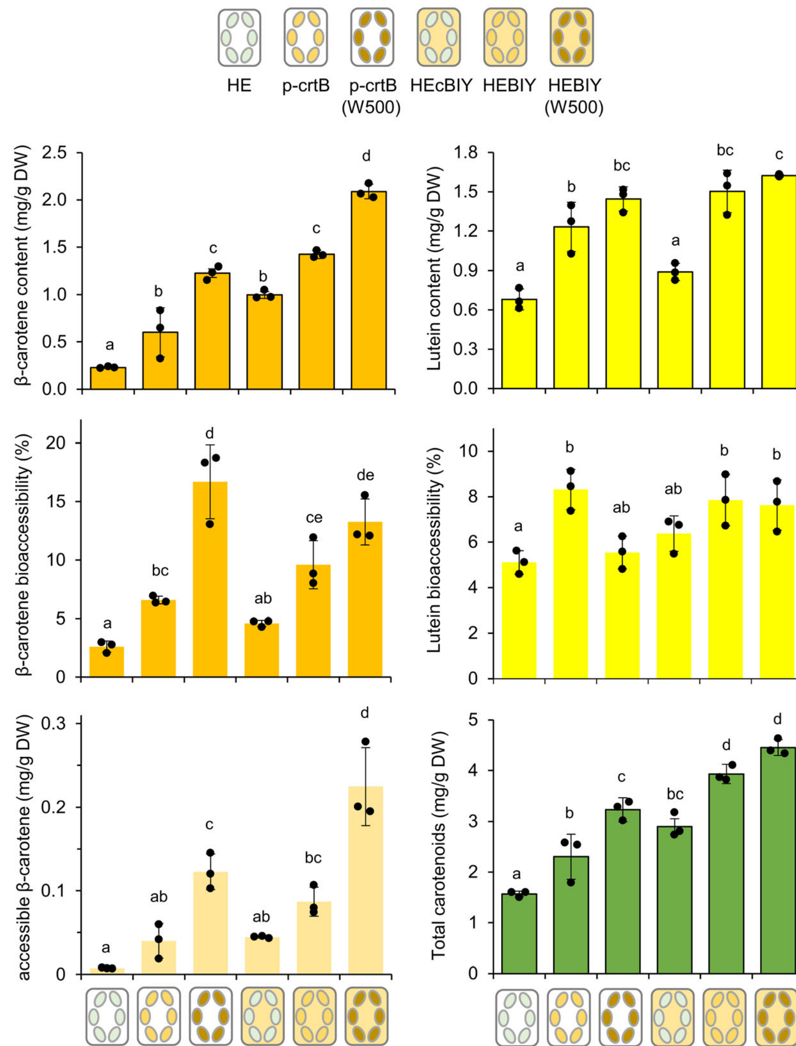

Figure 7. Subcellular accumulation impacts β-carotene bioaccessibility.
N. benthamiana plants grown under normal light conditions (W50) were exposed for 3 days to 10-fold higher light intensity (W500) or kept under W50. Then, leaves from the two sets of plants were agroinfiltrated with the indicated construct combinations and analyzed at 6 dpi (see Figure 1 caption for the nomenclature of construct combinations). Plots show carotenoid levels, bioaccessibility, and accessible content as the mean and SD of $n = 3$ independent biological replicates. Dots represent individual values and letters indicate statistically significant differences ($P < 0.05$) among means.

GGPP synthase enzymes could efficiently convert the extra supply of MEP-derived IPP and DMAPP into GGPP and that the plastid-localized crtB enzyme was able to convert enhanced levels of GGPP into phytoene. However, the conversion of the extra phytoene into downstream carotenoids appeared to be limiting in *N. benthamiana* leaves. Several explanations for the observed poor phytoene conversion are possible. It is likely that biosynthetic and storage mechanisms could already be saturated in crtB-containing samples, thus limiting further increases upon enhancing the supply of phytoene. Most crtB-derived phytoene is produced and stored in PG, where it can be further converted into β-carotene (Morelli, Torres-Montilla, et al., 2023). However, it is also possible that the additional phytoene produced when SlDXS1 is added cannot be accessed by endogenous enzymes due to differential compartmentation. In any case, the upregulated production of phytoene was found to speed up the ϕPSII drop associated with the initial loss of chloroplast identity (Figure 3B), consistent with the proposed model that the accumulation of this carotenoid precursor is the main trigger of the artificial chromoplast differentiation process (Llorente et al., 2020). It is intriguing that only the tomato SlDXS1 isoform worked to produce more phytoene. SlDXS1 is the main isoform participating in carotenoid biosynthesis in tomato (also during fruit ripening, when carotenoid accumulation is boosted as chloroplasts differentiate into chromoplasts), while *SlDXS2* shows lower levels of expression in most

© 2024 The Author(s).

1365313x, 2024, 6, Downloaded from https://onlinelibrary.wiley.com/doi/10.1111/tpj.16964 by Universitat Politecnica De Valencia, Wiley Online Library on [19/09/2024]. See the Terms and Conditions (https://onlinelibrary.wiley.com/terms-and-conditions) on Wiley Online Library for rules of use; OA articles are governed by the applicable Creative Commons License

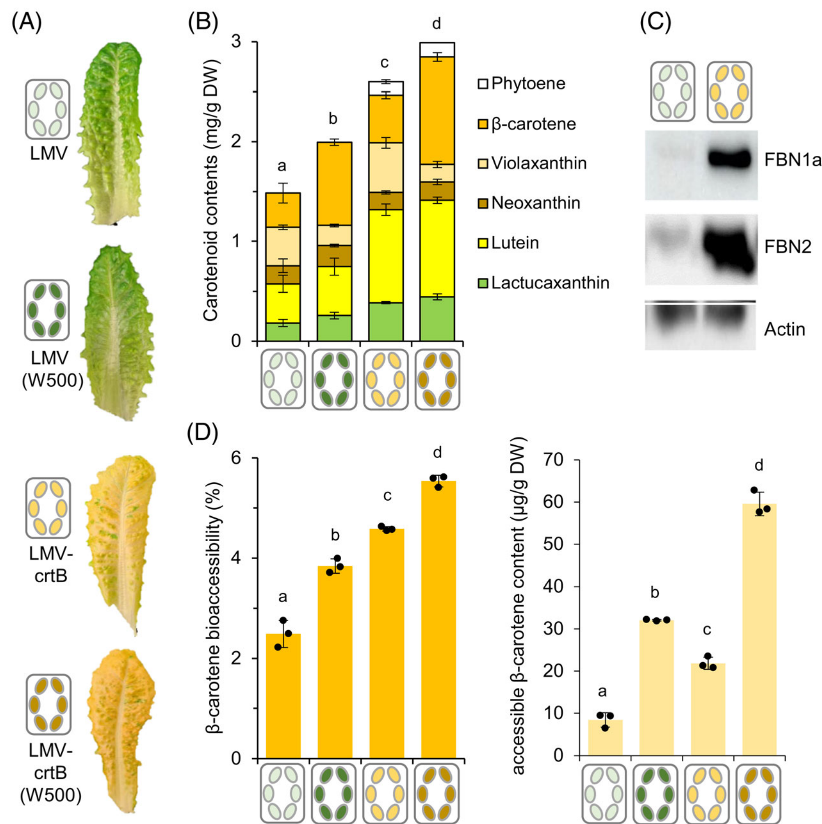

Figure 8. Higher-light treatment increases β-carotene contents and bioaccessibility in lettuce leaves.
Romaine lettuce plants grown under normal light conditions (W50) and inoculated with the indicated viral vectors were exposed for 5 days to 10-fold higher light intensity (W500) or kept under W50. After transferring them back to W50 for 2 days, leaves from the two sets of plants were collected and snap-frozen for further analysis.
(A) Representative images of collected leaves with a schematic presentation of treatments.
(B) Plot representing the mean and SD of carotenoid levels in $n = 3$ independent biological replicates per treatment.
(C) Immunoblot analysis of PG-associated protein markers (fibrillins FBN1a and FBN2) in the indicated samples. Actin levels were analyzed as loading controls.
(D) Bioaccessibility and accessible content of β-carotene in the samples analyzed in (B). Dots represent individual values and letters indicate statistically significant differences ($P < 0.05$) among means.

tissues but it is induced in specialized structures such as leaf trichomes in response to environmental stimuli to produce dedicated isoprenoids (Brand & Tissier, 2022; Lois et al., 2000; Paetzold et al., 2010). In the case of AtDXS, the only enzyme with DXS activity in Arabidopsis (Carretero-Paulet et al., 2013; Phillips et al., 2008), it can be argued that the SlDXS1 enzyme comes from tomato, and hence might work better in another species of the Solanaceae family—such as *N. benthamiana*—than an enzyme from the Brassicaceae family. In agreement with this possibility, the production of phytoene in Golden Rice (monocot) was highly increased when a monocot PSY (from maize) was used instead of the initial dicot PSY (from daffodil) enzyme (Paine et al., 2005). Alternatively, AtDXS and/or SlDXS2 might have a lower catalytic activity than SlDXS1, or they might interact with different partners. For example, it has been shown that the tomato chromoplast-associated PSY1 isoform is less active than the chloroplast-associated PSY2 (Cao et al., 2019), and these two enzymes can directly interact with the GGPP synthase isoform SlG2 but not with SlG3 (Barja et al., 2021) or SlG1 (Ezquerro et al., 2023).

Further attempts to improve strategy P besides increasing MEP pathway flux had a limited success. While the GA_3 treatment did slightly improve artificial chromoplast differentiation (Figure 4), it had deleterious effects in non-agroinfiltrated leaves and stems, which turned longer and paler. Also, the phytohormone treatment had to be performed in a specific moment after agroinfiltration (to avoid the formation of too much humidity on the agroinfiltration halo that could affect the efficiency of transformation), which makes it difficult to implement in large-scale production settings. These factors, together with regulatory constraints associated with the use of chemicals and the high economic cost of the treatment, prevent treating with gibberellins as a β-carotene biofortification method for commercial use. Alternatively, genetic manipulations of

© 2024 The Author(s).

1365313x, 2024, 6, Downloaded from https://onlinelibrary.wiley.com/doi/10.1111/tpj.16964 by Universitat Politecnica De Valencia, Wiley Online Library on [19/09/2024]. See the Terms and Conditions (https://onlinelibrary.wiley.com/terms-and-conditions) on Wiley Online Library for rules of use; OA articles are governed by the applicable Creative Commons License

the carotenoid pathway could help to increase β-carotene contents, as demonstrated here with the *lut2* mutant (Figure 5B). Higher enrichments would be expected by blocking the conversion of β-carotene into downstream xanthophylls (Figure 1A), which accumulate at high levels in the chromoplasts of *lut2* leaves (Figure 5A). The WT carotenoid phenotype of crtB-infected retrograde mutants such as *gun1* (Koussevitzky et al., 2007), *sal1* (Estavillo et al., 2011), and *csb3* (Xiao et al., 2012) indicates that chloroplast-to-chromoplast differentiation in Arabidopsis leaves can proceed normally despite the defective operation of at least some chloroplast-to-cytosol/nucleus signaling pathways. A related conclusion of our work is that the production of IPP and DMAPP for carotenoid synthesis by cytosolic (MVA) and plastidial (MEP) pathways is independent, i.e., both pathways can work together at the same time without interfering with each other, as deduced from the observation that combining strategies C and P results in an additive phenotype (Figure 1B). This novel information should open the door to engineer the production of isoprenoids of interest in plant biofactories by using not one but the two pathways supplying their metabolic precursors. Because the MVA and MEP pathways can be activated independently, they can also be used to boost the production of derived products (such as carotenoids) in multiple cell compartments at different times.

Lettuce is an excellent source of vitamins, minerals, and bioactive compounds such as polyphenols and carotenoids (Shi et al., 2022). Both agroinfiltration and viral vectors were previously demonstrated to work in lettuce to produce extraplastidial carotenoids by strategy C (Andersen et al., 2021) and to promote carotenoid accumulation by strategy P (Llorente et al., 2020; Morelli & Rodriguez-Concepcion, 2022). Here, we went a step forward by showing that both the accumulation and the bioaccessibility of β-carotene increase after inducing the proliferation of PGs in lettuce leaves either by strategy P or by just exposing unmodified leaves to stronger light (Figure 8). It is important to note that enriching carotenoid contents in a particular food is only the first step toward efficient biofortification. However, the vast majority of works aiming to improve the carotenoid content of plant products fail to confirm whether carotenoid intake from the engineered food is also improved (Morelli & Rodriguez-Concepcion, 2023). Carotenoids are lipophilic isoprenoids that must first be released from the food matrix and then incorporated into water-miscible intestinal micelles. The physicochemical contexts and subcellular locations where carotenoids accumulate in plant cells highly influence bioaccessibility (Watkins & Pogson, 2020; Zheng et al., 2020). Although a strong influence of light and other environmental conditions on the contents of these health-promoting phytonutrients has been reported in lettuce (He et al., 2021; Li et al., 2021; Samuolienė et al., 2021), the positive effect of PG differentiation on β-carotene accumulation and bioaccessibility was unknown. A correlation between PG storage and bioaccessibility has been shown for β-carotene and other carotenoids in several plant systems. For example, fruits containing abundant PGs such as mango and papaya showed a higher β-carotene bioaccessibility than fruits with chromoplasts with few or no PGs such as melon or grapefruit (Jeffery, Holzenburg, & King, 2012; Jeffery, Turner, & King, 2012). In the chloroplasts of green tissues, β-carotene is associated with the photosynthetic apparatus in tightly built pigment-protein complexes resulting in a more difficult release during digestion and a subsequent lower bioaccessibility compared to the pigment found in chromoplast vesicles such as PGs (Jeffery, Holzenburg, & King, 2012; Jeffery, Turner, & King, 2012; Lichtenthaler, 2007). Promoting PG proliferation with a higher-intensity light treatment (Van Wijk & Kessler, 2017) likely facilitates the accumulation of β-carotene in these subcompartments and hence improves bioaccessibility. The conclusion that PG localization enhances β-carotene bioaccessibility is indirectly supported by the unchanged bioaccessibility of lutein in PG-enriched W500 samples compared to W50 controls (Figure 7), since lutein does not accumulate in the PGs found in artificial leaf chromoplasts (Morelli, Torres-Montilla, et al., 2023). Additionally, PGs from artificial chromoplasts harbor higher levels of isoprenoid vitamins E (tocopherols) and K1 (phylloquinone), making them interesting structures to target for the nutritional enrichment of leaves (Morelli, García-Romañach, et al., 2023; Morelli, Torres-Montilla, et al., 2023).

The use of agroinfiltration, viral vectors, or specific promoters allows targeting specific leaf areas, tissues or developmental stages to trigger chromoplastogenesis, while preserving the photosynthetic capacity of the rest to support photosynthesis. In any case, there is still a long way to the commercial application of this technology. While advances in synthetic biology are permitting to deploy complex gene circuits in plants that activate upon chemical or physical treatments at appropriate tissues or developmental stages, reaching the market will strongly depend on the evolution of societal and political concerns toward genetic manipulation (Rodriguez-Concepcion & Daròs, 2022). Future developments to deliver nucleic acid sequences and proteins into plant cells without using bacterial or viral vectors may solve at least some of these limitations.

MATERIALS AND METHODS

Plant material and growth conditions

Arabidopsis thaliana wild-type (Columbia) and mutant alleles *gun1-101* (Llamas et al., 2017), *sal1/ron1-2* (Robles et al., 2010), *csb3/clb4-3* (Flores-Pérez et al., 2008), *vte1* (Porfirova et al., 2002), and *lut2* (Emiliani et al., 2018) were grown and infected with viral

1365313x, 2024, 6, Downloaded from https://onlinelibrary.wiley.com/doi/10.1111/tpj.16964 by Universitat Politecnica De Valencia, Wiley Online Library on [19/09/2024]. See the Terms and Conditions (https://onlinelibrary.wiley.com/terms-and-conditions) on Wiley Online Library for rules of use; OA articles are governed by the applicable Creative Commons License

vectors as described by Llorente et al. (2020). *Nicotiana benthamiana* and *Lactuca sativa* (var. Romaine) plants used for the transient expression assays were grown in a greenhouse under a stable photoperiod of 14 h of light (PPFD of 50 μmol m^{-2} sec^{-1} photons, referred to as W50) at 26°C and 10 h dark at 21°C. To promote PG proliferation with a more intense light treatment, 4-week-old *N. benthamiana* plants were moved to a Fitoclima 600 plant growth chamber (Aralab, Madrid, Spain) with the same photoperiod but higher PPFD (500 μmol m^{-2} sec^{-1} photons, W500) for 3 days. After agroinfiltration, plants were moved to the original light conditions (W50) to allow carotenoid production under normal conditions. In the case of lettuce, the times were adjusted to the slower growth rate of this species and the longer action time of viral vectors compared to agroinfiltrated constructs. Specifically, 3 leaves of 4-week-old plants were inoculated with *N. benthamiana* tissue infected with LMV-crtB or an empty vector LMV control (Llorente et al., 2020) in at least 6 different spots. About 6 days later (when the first symptoms of viral infection were visually detected), they were moved to W500 conditions for 5 days to promote PG proliferation. Then, plants were moved to W50 conditions for 2 additional days. For treatments with phytohormones and inhibitors, we diluted them in water and 0.05% Tween 20 (to lower surface tension and delay the evaporation of the solution) at the concentrations indicated in Table 2. As inhibitors, we used paclobutrazol to block endogenous gibberellin biosynthesis (Hedden & Graebe, 1985), the 4-hydroxyaryl hydroxamic acid D2 to inhibit strigolactone biosynthesis (Harrison et al., 2015), and L-kynurenine to inhibit auxin biosynthesis (He et al., 2011). The solutions were applied with a fine brush on the surface of *N. benthamiana* leaves 2 h after agroinfiltration (i.e., once the agroinfiltration halo was dried).

Gene constructs and transient expression assays

The *P. ananatis crtY* gene was cloned in the Gateway pGWB405 vector as described by Llorente et al. (2020). Similarly, cDNA sequences for AtDXS, SlDXS1, and SlDXS2 were amplified from Arabidopsis or tomato and cloned into pGWB405 (AtDXS), pGWB420 (SlDXS1), or pGWB454 (SlDXS2). Combinations of cultures of *Agrobacterium tumefaciens* GV3101 strains transformed with the resulting constructs and others overexpressing tHMGR, crtE, crtI and different versions of crtB (Andersen et al., 2021; Llorente et al., 2020) were infiltrated in *N. benthamiana* leaves (i.e., agroinfiltrated) as described by Andersen et al. (2021). All constructs were under the control of the constitutive *35S* promoter. Cultures were mixed in identical proportions for the various combinations. Unless indicated otherwise, agroinfiltrated leaf samples were collected at 6 days post-infiltration (dpi). Inoculation of Arabidopsis and lettuce plants with viral vectors was performed as described by Llorente et al. (2020).

Protoplast isolation

Agroinfiltrated areas of leaves at 6 dpi were cut into 0.5 cm-wide strips in a glass Petri dish with 5 ml of digestion solution: 10 mM MES pH 5.7, 1.5% (w/v) cellulase, 0.75% (w/v) macerozyme, 0.5 M mannitol, 1 mM $CaCl_2$. After incubation at room temperature for 5 h, aliquots were used for observation of leaf protoplasts using an Eclipse E600 microscope (Nikon Instruments Inc., Melville NY, USA).

Electron microscopy

Agroinfiltrated leaves were collected at 6-dpi and initially fixed using Karnovsky solution—2.5% (w/v) paraformaldehyde and 0.5% (w/v) glutaraldehyde—followed by three 5 min washes with 0.1 M phosphate buffer saline. Post-fixation was achieved by immersing the samples in 2% osmium tetroxide for 2 h, followed by three 5 min washes with water. Gradual dehydration steps were carried out at increasing temperatures (30, 50, 70, and 90°C). Subsequently, infiltration of the samples with LR-White resin was executed in different ethanol–resin mixtures (ranging from 1:2 to 1:1) at 90°C, followed by a final immersion in 100% LR-White resin for 1 to 24 h. Samples were then embedded in gelatin capsules, polymerized at 60°C for 48 h, and subsequently sectioned using holey grids. Contrast staining was performed using 2% (w/v) uranyl acetate for 9 min followed by lead citrate for 9 min. Samples were then visualized using an HT7800 120Kv TEM (Hitachi Ltd, Tokyo, Japan) and images were taken with a CMOS XAROSA digital camera of 20 Mpx (EMSIS GmbH, Münster, Germany).

Photosynthetic measurements

Chlorophyll fluorescence parameters were acquired with a Handy GFP Cam (Photon Systems Instruments, Drásov, Czech Republic) with the exception of the experiments reported in Figure 4, for which a MAXI-PAM fluorimeter (Heinz Walz GmbH, Effeltrich, Germany) was used. The effective quantum yield of PSII (ϕPSII), referred to as QY_Lss in the Handy GFP Cam and Y(II) in the MAXI-PAM, was measured in dark-adapted leaves and it corresponds to (Fm′-Fs)/Fm′, where Fm′ and Fs are the maximum and minimum fluorescence of light-exposed plants, respectively. A saturating pulse (SAT) of 800 msec with an intensity of 3920 μmol m^{-2} sec^{-1} was used in the case of the Handy GFP Cam, whereas a slightly shorter SAT (720 msec) and higher intensity (4800 μmol m^{-2} sec^{-1}) was used with the MAXI-PAM. The chosen light intensity to excite the basal level of fluorescence was 21 μmol m^{-2} sec^{-1} photons in all cases, as this was established as the optimal intensity causing a measurable difference between Fo and Fm according to our previous studies of leaf chromoplastogenesis (Llorente et al., 2020).

In vitro bioaccessibility assay

The *in vitro* digestion procedure was performed as described by Morelli and Rodriguez-Concepcion (2022). Briefly, *N. benthamiana* leaves were agroinfiltrated with HE (a control for β-carotene exclusively present in chloroplasts), p-crtB (in which β-carotene is stored in the PG of artificial chromoplasts), HEcBlY (with β-carotene accumulated in chloroplasts and extraplastidial locations) or HEBlY (in which β-carotene is accumulated in artificial chromoplasts and extraplastidial locations). At 6 dpi, samples were collected and used to estimate the percentage of carotenoids remaining in the tissue after *in vitro* digestion. The digested and undigested samples were analyzed by HPLC as described by Barja et al. (2021). Bioaccessibility was calculated as the ratio between carotenoid concentration after digestion and the concentration of the same compound in the starting undigested sample. Accessible carotenoid contents were calculated by multiplying the amount of carotenoid in the sample by the corresponding bioaccessibility percentage.

Protein and metabolite analysis

Carotenoids and chlorophylls were extracted and analyzed by HPLC as described by Barja et al. (2021). Protein extraction and separation were carried out as described by Morelli, Torres-Montilla et al. (2023) using approximately 5 mg of freeze-dried leaf tissue. For immunoblot analysis, primary antibodies against FBN1A, FBN2, and actin and a secondary antibody conjugated with horseradish peroxidase (Millipore) were used. Detection of immunoreactive bands was performed using SuperSignal West Pico PLUS (Thermo Fisher Scientific, Waltham MA, USA).

© 2024 The Author(s).

1365313x, 2024, 6, Downloaded from https://onlinelibrary.wiley.com/doi/10.1111/tpj.16964 by Universitat Politecnica De Valencia, Wiley Online Library on [19/09/2024]. See the Terms and Conditions (https://onlinelibrary.wiley.com/terms-and-conditions) on Wiley Online Library for rules of use; OA articles are governed by the applicable Creative Commons License

Chemiluminescent signals were visualized using an ImageQuant 800 biomolecular imager (Amersham, Little Chalfont, UK).

Statistical analyses

One-way ANOVA followed by Tukey's multiple comparisons test and Student's *t*-test analyses available in the GraphPad and Microsoft Excel packages were used to determine statistically significant differences. For measurement of metabolite (carotenoid) levels, we collected agroinfiltrated areas from three or more independent *N. benthamiana* leaves, each from a different plant ($n \geq 3$), or infected leaves of three individual Arabidopsis or lettuce plants ($n = 3$). Photosynthetic parameters were measured in several points within the agroinfiltrated areas of at least three independent leaves, each from a different plant ($n \geq 3$). Further details of experimental design and sampling can be found in figure captions.

AUTHOR CONTRIBUTIONS

LM, PP-C, and MR-C conceived the project and designed the experiments. BL generated constructs. LM, PP-C, DR-L, and XD conducted the experiments and analyzed the data. LM, PP-C, BL, and MR-C discussed the results, LM and MR-C wrote the paper. All authors reviewed the manuscript.

ACKNOWLEDGMENTS

We thank Trine B. Andersen and Jose A. Daros for materials, José Luis Micol for the *ron1-2* mutant, Felix Kessler for the *vte1* mutant, Alberto Coronado-Martín for help with protoplast isolation, and M. Rosa Rodriguez, Jose Perez-Beser and the staff at the IBMCP Metabolomics Platform for technical support. We also thank the Microscopy Section at the University of Valencia SCSIE and Maria T. Mínguez for her specialized support with electron microscopy. This work was funded by grants from Spanish MCI-N/AEI/10.13039/501100011033 and European NextGeneration EU/PRTR and PRIMA programs to MR-C (PID2020-115810GB-I00 and UToPIQ-PCI2021-121941). MR-C is also supported by Generalitat Valenciana (PROMETEU/2021/056 and AGROALNEXT/2022/067) and the MCIN/AEI-funded Spanish Carotenoid Network, CaRed (RED2022-134577-T). BL acknowledges the support of the Gordon and Betty Moore Foundation (GBMF9319, grant DOI: https://doi.org/10.37807/GBMF9319), the ARC Centre of Excellence for Synthetic Biology, Twist Bioscience, and the Allen Foundation. LM and PP-C received predoctoral fellowships from La Caixa Foundation (INPhINIT program LCF/BQ/IN18/11660004) and Generalitat Valenciana (CIACIF/2021/278), respectively.

CONFLICT OF INTEREST STATEMENT

The authors declare that there is no conflict of interest.

DATA AVAILABILITY STATEMENT

All relevant data can be found within the manuscript. Raw data are available upon request.

REFERENCES

Andersen, T.B., Llorente, B., Morelli, L., Torres-Montilla, S., Bordanaba-Florit, G., Espinosa, F.A. *et al.* (2021) An engineered extraplastidial pathway for carotenoid biofortification of leaves. *Plant Biotechnology Journal*, **19**, 1008–1021.

Barja, M.V., Ezquerro, M., Beretta, S., Diretto, G., Florez-Sarasa, I., Feixes, E. *et al.* (2021) Several geranylgeranyl diphosphate synthase isoforms supply metabolic substrates for carotenoid biosynthesis in tomato. *The New Phytologist*, **231**, 255–272.

Brand, A. & Tissier, A. (2022) Control of resource allocation between primary and specialized metabolism in glandular trichomes. *Current Opinion in Plant Biology*, **66**, 102172.

Britton, G. (1995) Structure and properties of carotenoids in relation to function. *The FASEB Journal*, **9**, 1551–1558.

Bu, X., Lin, J.Y., Duan, C.Q., Koffas, M.A.G. & Yan, G.L. (2022) Dual regulation of lipid droplet-triacylglycerol metabolism and ERG9 expression for improved b-carotene production in *Saccharomyces cerevisiae*. *Microbial Cell Factories*, **21**, 3–13.

Cao, H., Luo, H., Yuan, H., Eissa, M.A., Thannhauser, T.W., Welsch, R. *et al.* (2019) A neighboring aromatic-aromatic amino acid combination governs activity divergence between tomato phytoene synthases. *Plant Physiology*, **180**, 1988–2003.

Carretero-Paulet, L., Cairó, A., Talavera, D., Saura, A., Imperial, S., Rodríguez-Concepción, M. *et al.* (2013) Functional and evolutionary analysis of DXL1, a non-essential gene encoding a 1-deoxy-D-xylulose 5-phosphate synthase like protein in *Arabidopsis thaliana*. *Gene*, **524**, 40–53.

Díaz-Gómez, J., Twyman, R.M., Zhu, C., Farré, G., Serrano, J.C., Portero-Otin, M. *et al.* (2017) Biofortification of crops with nutrients: factors affecting utilization and storage. *Current Opinion in Biotechnology*, **44**, 115–123.

Domonkos, I., Kis, M., Gombos, Z. & Ughy, B. (2013) Carotenoids, versatile components of oxygenic photosynthesis. *Progress in Lipid Research*, **52**, 539–561.

Emiliani, J., D'Andrea, L., Falcone Ferreyra, M.L., Maulión, E., Rodríguez, E., Rodríguez-Concepción, M. *et al.* (2018) A role for β,β-xanthophylls in Arabidopsis UV-B photoprotection. *Journal of Experimental Botany*, **69**, 4921–4933.

Estavillo, G.M., Crisp, P.A., Pornsiriwong, W., Wirtz, M., Collinge, D., Carrie, C. *et al.* (2011) Evidence for a SAL1-PAP chloroplast retrograde pathway that functions in drought and high light signaling in Arabidopsis. *Plant Cell*, **23**, 3992–4012.

Esteban, R., Barrutia, O., Artetxe, U., Fernández-Marín, B., Hernández, A. & García-Plazaola, J.I. (2015) Internal and external factors affecting photosynthetic pigment composition in plants: a meta-analytical approach. *The New Phytologist*, **206**, 268–280.

Ezquerro, M., Li, C., Pérez-Pérez, J., Burbano-Erazo, E., Barja, M.V., Wang, Y. *et al.* (2023) Tomato geranylgeranyl diphosphate synthase isoform 1 is involved in the stress-triggered production of diterpenes in leaves and strigolactones in roots. *The New Phytologist*, **239**, 2292–2306.

Ezzedine, J.A., Uwizeye, C., Si Larbi, G., Villain, G., Louwagie, M., Schilling, M. *et al.* (2023) Adaptive traits of cysts of the snow alga *Sanguina nivaloides* unveiled by 3D subcellular imaging. *Nature Communications*, **14**, 7500.

Mi, J., Vallarino, J.G., Petřík, I., Novák, O., Correa, S.M., Chodasiewicz, M., *et al.* (2022) A manipulation of carotenoid metabolism influence biomass partitioning and fitness in tomato. *Metab. Eng.*, **70**, 166–180.

Fitzpatrick, T.B., Basset, G.J.C., Borel, P., Carrari, F., DellaPenna, D., Fraser, P.D. *et al.* (2012) Vitamin deficiencies in humans: can plant science help? *Plant Cell*, **24**, 395–414.

Flores-Pérez, U., Pérez-Gil, J., Rodríguez-Villalón, A., Gil, M.J., Vera, P. & Rodríguez-Concepción, M. (2008) Contribution of hydroxymethylbutenyl diphosphate synthase to carotenoid biosynthesis in bacteria and plants. *Biochemical and Biophysical Research Communications*, **371**, 510–514.

Gopal, S.S., Lakshmi, M.J., Sharavana, G., Sathaiah, G., Sreerama, Y.N. & Baskaran, V. (2017) Lactucaxanthin-a potential anti-diabetic carotenoid from lettuce (*Lactuca sativa*) inhibits α-amylase and α-glucosidase activity in vitro and in diabetic rats. *Food & Function*, **8**, 1124–1131.

Harrison, P.J., Newgas, S.A., Descombes, F., Shepherd, S.A., Thompson, A.J. & Bugg, T.D.H. (2015) Biochemical characterization and selective inhibition of β-carotene cis-trans isomerase D27 and carotenoid cleavage dioxygenase CCD8 on the strigolactone biosynthetic pathway. *The FEBS Journal*, **282**, 3986–4000.

Hashimoto, H., Uragami, C., Yukihira, N., Gardiner, A.T. & Cogdell, R.J. (2018) Understanding/unravelling carotenoid excited singlet states. *Journal of the Royal Society Interface*, **15**, 20180026.

He, J., Jawahir, N.K.B. & Qin, L. (2021) Quantity of supplementary LED lightings regulates photosynthetic apparatus, improves photosynthetic

© 2024 The Author(s).

1365313x, 2024, 6, Downloaded from https://onlinelibrary.wiley.com/doi/10.1111/tpj.16964 by Universitat Politecnica De Valencia, Wiley Online Library on [19/09/2024]. See the Terms and Conditions (https://onlinelibrary.wiley.com/terms-and-conditions) on Wiley Online Library for rules of use; OA articles are governed by the applicable Creative Commons License

capacity and enhances productivity of cos lettuce grown in a tropical greenhouse. *Photosynthesis Research*, **149**, 187–199.

He, W., **Brumos, J.**, **Li, H.**, **Ji, Y.**, **Ke, M.**, **Gong, X.** ***et al.*** (2011) A small-molecule screen identifies L-kynurenine as a competitive inhibitor of TAA1/TAR activity in ethylene-directed auxin biosynthesis and root growth in Arabidopsis. *Plant Cell*, **23**, 3944–3960.

Hedden, P. & **Graebe, J.E.** (1985) Inhibition of gibberellin biosynthesis by paclobutrazol in cell-free homogenates of *Cucurbita maxima* endosperm and *Malus pumila* embryos. *Journal of Plant Growth Regulation*, **4**, 111–122.

Jeffery, J., **Holzenburg, A.** & **King, S.** (2012) Physical barriers to carotenoid bioaccessibility. Ultrastructure survey of chromoplast and cell wall morphology in nine carotenoid-containing fruits and vegetables. *Journal of the Science of Food and Agriculture*, **92**, 2594–2602.

Jeffery, J.L., **Turner, N.D.** & **King, S.R.** (2012) Carotenoid bioaccessibility from nine raw carotenoid-storing fruits and vegetables using an in vitro model. *Journal of the Science of Food and Agriculture*, **92**, 2603–2610.

Kim, J.E., **Rensing, K.H.**, **Douglas, C.J.** & **Cheng, K.M.** (2010) Chromoplasts ultrastructure and estimated carotene content in root secondary phloem of different carrot varieties. *Planta*, **231**, 549–558.

Koussevitzky, S., **Nott, A.**, **Mockler, T.C.**, **Hong, F.**, **Sachetto-Martins, G.**, **Surpin, M.** ***et al.*** (2007) Signals from chloroplasts converge to regulate nuclear gene expression. *Science*, **316**, 715–719.

Li, Y., **Wu, L.**, **Jiang, H.**, **He, R.**, **Song, S.**, **Su, W.** ***et al.*** (2021) Supplementary far-red and blue lights influence the biomass and phytochemical profiles of two lettuce cultivars in plant factory. *Molecules*, **26**, 7405.

Lichtenthaler, H.K. (2007) Biosynthesis, accumulation and emission of carotenoids, α-tocopherol, plastoquinone, and isoprene in leaves under high photosynthetic irradiance. *Photosynthesis Research*, **92**, 163–179.

Lichtenthaler, H.K. (2012) Biosynthesis, localization and concentration of carotenoids in plants and algae. In Eaton-Rye, J., Tripathy, B., & Sharkey, T. (Eds.), *Photosynthesis. Advances in Photosynthesis and Respiration*, vol. **34**. Dordrecht: Springer. https://doi.org/10.1007/978-94-007-1579-0_4

Llamas, E., **Pulido, P.** & **Rodríguez-Concepción, M.** (2017) Interference with plastome gene expression and Clp protease activity in Arabidopsis triggers a chloroplast unfolded protein response to restore protein homeostasis. *PLoS Genetics*, **13**, e1007022.

Llorente, B., **Torres-Montilla, S.**, **Morelli, L.**, **Florez-Sarasa, I.**, **Matus, J.T.**, **Ezquerro, M.** ***et al.*** (2020) Synthetic conversion of leaf chloroplasts into carotenoid-rich plastids reveals mechanistic basis of natural chromoplast development. *Proceedings of the National Academy of Sciences of the United States of America*, **117**, 21796–21803.

Lois, L.M., **Rodríguez-Concepción, M.**, **Gallego, F.**, **Campos, N.** & **Boronat, A.** (2000) Carotenoid biosynthesis during tomato fruit development: regulatory role of 1-deoxy-D-xylulose 5-phosphate synthase. *The Plant Journal*, **22**, 503–513.

Majer, E., **Llorente, B.**, **Rodríguez-Concepción, M.** & **Daròs, J.A.** (2017) Rewiring carotenoid biosynthesis in plants using a viral vector. *Scientific Reports*, **7**, 41645.

Morelli, L., **García Romañach, L.**, **Glauser, G.**, **Shanmugabalaji, V.**, **Kessler, F.** & **Rodriguez-Concepcion, M.** (2023) Nutritional enrichment of plant leaves by combining genes promoting tocopherol biosynthesis and storage. *Metabolites*, **13**, 193.

Morelli, L. & **Rodriguez-Concepcion, M.** (2022) A fast and simplified method to estimate bioaccessibility of carotenoids from plant tissues. *Methods in Enzymology*, **674**, 329–341.

Morelli, L. & **Rodriguez-Concepcion, M.** (2023) Open avenues for carotenoid biofortification of plant tissues. *Plant Communications*, **4**, 100466.

Morelli, L., **Torres-Montilla, S.**, **Glauser, G.**, **Shanmugabalaji, V.**, **Kessler, F.** & **Rodriguez-Concepcion, M.** (2023) Novel insights into the contribution of plastoglobules and reactive oxygen species to chromoplast differentiation. *The New Phytologist*, **237**, 1696–1710.

Nogueira, M., **Mora, L.**, **Enfissi, E.M.A.**, **Bramley, P.M.** & **Fraser, P.D.** (2013) Subchromoplast sequestration of carotenoids affects regulatory mechanisms in tomato lines expressing different carotenoid gene combinations. *Plant Cell*, **25**, 4560–4579.

Paetzold, H., **Garms, S.**, **Bartram, S.**, **Wieczorek, J.**, **Urós-Gracia, E.M.**, **Rodríguez-Concepción, M.** ***et al.*** (2010) The isogene 1-deoxy-D-xylulose 5-phosphate synthase 2 controls isoprenoid profiles, precursor pathway allocation, and density of tomato trichomes. *Molecular Plant*, **3**, 904–916.

Paine, J.A., **Shipton, C.A.**, **Chaggar, S.**, **Howells, R.M.**, **Kennedy, M.J.**, **Vernon, G.** ***et al.*** (2005) Improving the nutritional value of Golden Rice through increased pro-vitamin a content. *Nature Biotechnology*, **23**, 482–487.

Pascal, A.A., **Liu, Z.**, **Broess, K.**, **Van Oort, B.**, **Van Amerongen, H.**, **Wang, C.** ***et al.*** (2005) Molecular basis of photoprotection and control of photosynthetic light-harvesting. *Nature*, **436**, 134–137.

Phillip, D. & **Young, A.J.** (1995) Occurrence of the carotenoid lactucaxanthin in higher plant LHC II. *Photosynthesis Research*, **43**, 273–282.

Phillips, M.A., **León, P.**, **Boronat, A.** & **Rodríguez-Concepción, M.** (2008) The plastidial MEP pathway: unified nomenclature and resources. *Trends in Plant Science*, **13**, 619–623.

Pick, U., **Zarka, A.**, **Boussiba, S.** & **Davidi, L.** (2019) A hypothesis about the origin of carotenoid lipid droplets in the green algae Dunaliella and Haematococcus. *Planta*, **249**, 31–47.

Porfirova, S., **Bergmuller, E.**, **Tropf, S.**, **Lemke, R.** & **Dormann, P.** (2002) Isolation of an Arabidopsis mutant lacking vitamin E and identification of a cyclase essential for all tocopherol biosynthesis. *Proceedings of the National Academy of Sciences of the United States of America*, **99**, 12495–12500.

Ravanello, M.P., **Ke, D.**, **Alvarez, J.**, **Huang, B.** & **Shewmaker, C.K.** (2003) Coordinate expression of multiple bacterial carotenoid genes in canola leading to altered carotenoid production. *Metabolic Engineering*, **5**, 255–263.

Robles, P., **Fleury, D.**, **Candela, H.**, **Cnops, G.**, **Alonso-Peral, M.**, **Anami, S.** ***et al.*** (2010) The RON1/FRY1/SAL1 gene is required for leaf morphogenesis and venation patterning in Arabidopsis. *Plant Physiology*, **152**, 1357–1372.

Rodriguez-Concepcion, M., **Avalos, J.**, **Bonet, M.L.**, **Boronat, A.**, **Gomez-Gomez, L.**, **Hornero-Mendez, D.** ***et al.*** (2018) A global perspective on carotenoids: metabolism, biotechnology, and benefits for nutrition and health. *Progress in Lipid Research*, **70**, 62–93.

Rodríguez-Concepción, M. & **Boronat, A.** (2002) Elucidation of the methylerythritol phosphate pathway for isoprenoid biosynthesis in bacteria and plastids. A metabolic milestone achieved through genomics. *Plant Physiology*, **130**, 1079–1089.

Rodríguez-Concepción, M. & **Boronat, A.** (2015) Breaking new ground in the regulation of the early steps of plant isoprenoid biosynthesis. *Current Opinion in Plant Biology*, **25**, 17–22.

Rodriguez-Concepcion, M. & **Daròs, J.A.** (2022) Transient expression systems to rewire plant carotenoid metabolism. *Current Opinion in Plant Biology*, **66**, 102190.

Sadali, N.M., **Sowden, R.G.**, **Ling, Q.** & **Jarvis, R.P.** (2019) Differentiation of chromoplasts and other plastids in plants. *Plant Cell Reports*, **38**, 803–818.

Samuolienė, G., **Viršilė, A.**, **Miliauskienė, J.**, **Haimi, P.J.**, **Laužikė, K.**, **Brazaitytė, A.** ***et al.*** (2021) The physiological response of lettuce to red and blue light dynamics over different photoperiods. *Frontiers in Plant Science*, **11**, 610174.

Schweiggert, R.M., **Mezger, D.**, **Schimpf, F.**, **Steingass, C.B.** & **Carle, R.** (2012) Influence of chromoplast morphology on carotenoid bioaccessibility of carrot, mango, papaya, and tomato. *Food Chemistry*, **135**, 2736–2742.

Shi, M., **Gu, J.**, **Wu, H.**, **Rauf, A.**, **Emran, T.B.**, **Khan, Z.** ***et al.*** (2022) Phytochemicals, nutrition, metabolism, bioavailability, and health benefits in lettuce-a comprehensive review. *Antioxidants*, **11**, 1158.

Sun, T., **Yuan, H.**, **Cao, H.**, **Yazdani, M.**, **Tadmor, Y.** & **Li, L.** (2018) Carotenoid metabolism in plants: the role of plastids. *Molecular Plant*, **11**, 58–74.

Torres-Montilla, S. & **Rodriguez-Concepcion, M.** (2021) Making extra room for carotenoids in plant cells: new opportunities for biofortification. *Progress in Lipid Research*, **84**, 101128.

Van Wijk, K.J. & **Kessler, F.** (2017) Plastoglobuli: plastid microcompartments with integrated functions in metabolism, plastid developmental transitions, and environmental adaptation. *Annual Review of Plant Biology*, **68**, 253–289.

Watkins, J.L. & **Pogson, B.J.** (2020) Prospects for carotenoid biofortification targeting retention and catabolism. *Trends in Plant Science*, **25**, 501–512.

Welsch, R. & **Li, L.** (2022) Golden Rice-lessons learned for inspiring future metabolic engineering strategies and synthetic biology solutions. *Methods in Enzymology*, **671**, 1–29.

Xiao, Y., **Savchenko, T.**, **Baidoo, E.E.K.**, **Chehab, W.E.**, **Hayden, D.M.**, **Tolstikov, V.** ***et al.*** (2012) Retrograde signaling by the plastidial metabolite

© 2024 The Author(s).
The Plant Journal published by Society for Experimental Biology and John Wiley & Sons Ltd.,

1365313x, 2024, 6, Downloaded from https://onlinelibrary.wiley.com/doi/10.1111/tpj.16964 by Universitat Politecnica De Valencia, Wiley Online Library on [19/09/2024]. See the Terms and Conditions (https://onlinelibrary.wiley.com/terms-and-conditions) on Wiley Online Library for rules of use; OA articles are governed by the applicable Creative Commons License

MEcPP regulates expression of nuclear stress-response genes. *Cell*, **149**, 1525–1535.

Ye, X., **Al-Babili, S.**, **Klöti, A.**, **Zhang, J.**, **Lucca, P.**, **Beyer, P.** ***et al.*** (2000) Engineering the provitamin a (β-carotene) biosynthetic pathway into (carotenoid-free) rice endosperm. *Science*, **287**, 303–305.

Zhen, S. & **van Iersel, M.W.** (2017) Far-red light is needed for efficient photochemistry and photosynthesis. *Journal of Plant Physiology*, **209**, 115–122.

Zheng, X., **Giuliano, G.** & **Al-Babili, S.** (2020) Carotenoid biofortification in crop plants: citius, altius, fortius. *Biochimica et Biophysica Acta-Molecular and Cell Biology of Lipids*, **1865**, 158664.

Zheng, X., **Zhang, Y.**, **Balakrishna, A.**, **Liew, K.X.**, **Kuijer, H.N.J.**, **Xiao, T.T.** ***et al.*** (2023) Installing the Neurospora carotenoid pathway in plants enables cytosolic formation of provitamin a and its sequestration in lipid droplets. *Molecular Plant*, **16**, 1066–1081.

© 2024 The Author(s).
The Plant Journal published by Society for Experimental Biology and John Wiley & Sons Ltd.,

1365313x, 2024, 6, Downloaded from https://onlinelibrary.wiley.com/doi/10.1111/tpj.16964 by Universitat Politecnica De Valencia, Wiley Online Library on [19/09/2024]. See the Terms and Conditions (https://onlinelibrary.wiley.com/terms-and-conditions) on Wiley Online Library for rules of use; OA articles are governed by the applicable Creative Commons License